

**Electronic Supplementary Material (ESI)**

**Construction of supramolecular antibacterial material based on water-soluble pillar[5]arene and zwitterionic guest**

Haoming Liu,<sup>a</sup> Jinmeng Lv,<sup>a</sup> Xue Wang, Shengyi Dong,<sup>\*c</sup> Xinyun Li<sup>\*b</sup> and Lingyan Gao<sup>\*a</sup>

<sup>a</sup>Key Laboratory of Synthetic and Natural Functional Molecule Chemistry of the Ministry of Education, College of Chemistry and Materials Science, Northwest University, Xi'an China. E-mail: gaolingyan@nwu.edu.cn.

<sup>b</sup>College of Rehabilitation, Hangzhou Medical College, Hangzhou, China. E-mail: lxyjasmine2010@163.com.

<sup>c</sup>College of Chemistry and Chemical Engineering, Hunan University, Changsha 410082, China. E-mail: dongsy@hnu.edu.cn.

## Table of Contents

1. General	S1
2. Stoichiometric ratio of <b>H</b> and <b>G</b> in the host–guest <b>HG</b> complex	S1
3. Evaluation of antibacterial ability	S2
4. Evaluation of biofilm inhibition	S2
5. General procedures for bacterial biofilm formation and harvesting	S3
6. Evaluation of biofilm eradication	S3
7. Scanning electron microscopy (SEM)	S3
8. Cytoplasmic membrane potential assay	S4
9. Zeta potential measurements	S4
10. N-phenyl-naphthylamine (NPN) uptake assay	S4
11. Propidium iodide (PI) uptake assay	S5
12. Protein and DNA leakage assays	S5
13. Hemolysis assay	S5
14. Cell viability assay	S6
15. Statistical analysis	S6
Reference	S23

## 1. General

All reagents were commercially available and used as supplied without further purification. Compounds  $H^{S1}$  and  $G^{S2}$  were prepared according to the published procedures. The deionized water used was purified using a Millipore water purification system with a minimum resistivity of 18.0 M $\Omega$ cm. NMR spectra were recorded on a Bruker AVANCE III-400 MHz spectrometer at 298 K. Mass spectra were recorded on a Bruker ESI-Q-TOF II spectrometer. UV-vis spectroscopic studies were carried on Agilent Technologies Cary 100 UV-vis. Dynamic light scattering (DLS) was performed on a Malvern Nanosizer S instrument. Scanning electron microscope (SEM) images were collected on a Hitachi SU8010. The optical density was measured using a microplate reader on a THERMO Varioskan Flash.

Gram-negative strain *Escherichia coli* (*E. coli*, ATCC25922), Gram-positive strain *Staphylococcus aureus* (*S. aureus*, ATCC25923) and methicillin-resistant *Staphylococcus aureus* (MRSA, ATCC 43300) were adopted in this study. The bacteria were initially streaked from a -20 °C glycerol storage solution on a lysogen-based broth (Luria–Bertani broth (LB) and Tryptic Soy Broth (TSB)). After growing on LB or TSB agar plates, the cells were cultured from a fresh single colony in LB or TSB. All experiments were conducted at 37 °C. All glassware used in this study were sterilized before the test.

## 2. Stoichiometric ratio of H and G in the host–guest complex HG

To evaluate the stoichiometric ratio of **H** and **G** in water, we use a job plot method. **H** and **G** were dissolved in methanol solution, respectively. The methanol solutions of **H** and **G** were mixed together to obtain a series of solutions with different molar ratios of **H** and **G**, and the total concentration of **H** and **G** were kept as constant. Then the solvent in these solutions were completely removed and redissolved in water with the same volume as methanol. These aqueous solutions with different molar ratios of **H** and **G** were measured by UV-vis spectroscopy to determine the stoichiometric ratio of **H** and **G**.

### 3. Evaluation of antibacterial ability

Bacterial suspensions of *E. coli*, *S. aureus* and MRSA used for antibacterial tests were  $10^6$  CFU/mL (CFU represents the colony forming unit) in LB and TSB, respectively. 2-Fold serial dilutions of **H**, **G** and **HG** (100  $\mu$ L) were prepared in a microdilution plate. Then 100  $\mu$ L of bacterial suspension was added to each well. The cultures and samples were then incubated in an incubator at 37 °C for 24 h. The optical density at a wavelength of 600 nm ( $OD_{600}$ ) of the microdilution plate was read to determine the MIC values.

### 4. Evaluation of biofilm inhibition

*E. coli*, *S. aureus* and MRSA bacterial suspensions ( $OD_{600} = 1$ ) were used in the antibacterial test. For the bacterial growth of *E. coli*, 100  $\mu$ L of serial 1:2 dilutions of **H**, **G** and **HG** were prepared in flat-bottomed 96-well microplates. Control wells with no compound and wells without bacteria containing each tested concentration of the compounds (blanks) were also prepared. An equal volume (100  $\mu$ L) of bacterial suspension diluted 1:10 ( $OD_{600} = 0.1$ ) in LB was added to each well. After incubation for 24 h at 37 °C, free-floating bacteria and medium were removed by turning over the plates. The wells were vigorously rinsed at least four times with doubly distilled water (DDW). Next, 0.4% crystal violet (200  $\mu$ L) was added to each well. After 45 min, wells were vigorously rinsed three times with DDW to remove unbound dye. After adding 200  $\mu$ L of 30% acetic acid to each well, the plate was shaken for 15 min to release the dye. Biofilm formation was quantified by measuring the difference between the absorbance of untreated and treated bacterial samples for each tested concentration of the compounds and the absorbance of appropriate blank well at 492 nm using a microplate reader. Each concentration was tested in triplicates, and experiments were repeated three times. The biofilm inhibition abilities of **H**, **G** and **HG** against *S. aureus* and MRSA were performed as described previously with minor modifications, only with the change of culture medium from LB to TSB.

## **5. General procedures for bacterial biofilm formation and harvesting**

*E. coli* suspension of LB medium ( $10^8$  CFU/mL, 200  $\mu$ L) was added to the 96-well plate, and the 96-well plate was placed in an incubator and cultured at 37 °C for 24 h. The aged medium was replaced with fresh LB medium, and the corresponding biofilm was used for further biofilm eradication experiments. Each concentration was tested 3 times and the experiment was repeated 3 times. Bacterial growth of *S. aureus* or MRSA was only in medium changed from LB to TSB.

## **6. Evaluation of biofilm eradication**

The prefabricated 24h-old biofilms were treated with 200  $\mu$ L of **H**, **G** and **HG** respectively, and further incubated at 37 °C for 24 h. Then, the wells were gently rinsed three times with doubly distilled water (DDW). Next, 0.4% crystal violet (200  $\mu$ L) was added to each well. After 45 min, wells were vigorously rinsed three times with DDW to remove unbound dye. Following, 200  $\mu$ L of 30% acetic acid was added to each well and the plate was shaken for 15 min to release the dye. Biofilms were quantified by measuring the absorbance at 492 nm using a microplate reader. Each concentration was tested in triplicates, and experiments were repeated three times.

## **7. Scanning electron microscopy (SEM)**

The bacterial solution was co-cultured with **H**, **G** and **HG** in phosphate buffer solution (PBS) at 37 °C for 3 hours. The treated bacteria were washed with PBS twice and were fixed with 4% glutaraldehyde overnight at 4 °C. Then the bacteria were washed with sterile PBS, sequentially dehydrated by different contents of ethanol (30, 50, 70, 80, 90, 95, and 100%) for 10 min, respectively. The final samples were dropped onto a silicon wafer and then dried in a vacuum condition overnight. The specimens were coated with platinum before observation.

## **8. Cytoplasmic membrane potential assay**

The cytoplasmic membrane potential changes were conducted in the presence of a membrane potential-sensitive fluorescent dye of DiSC<sub>3</sub>(5). First, *E. coli* and *S. aureus*

suspensions were diluted with HEPES buffer (5 mM) to  $10^7$  CFU/mL, DiSC<sub>3</sub>(5) solution (0.8  $\mu$ M) was prepared with deionized water. Then 100  $\mu$ L of bacterial solution and 100  $\mu$ L of DiSC<sub>3</sub>(5) solution were incubated together until a stable value of fluorescence intensity was achieved. Then, 100  $\mu$ L of KCl solution (15 mM) was added to equilibrate the cytoplasmic and external K<sup>+</sup> ions. Subsequently, 50  $\mu$ L of bacterial suspension and 100  $\mu$ L of **H**, **G** and **HG**, respectively, were mixed in a 96 well plate to desired concentrations to be tested. *E. coli* or *S. aureus* with 1% Triton X-100 and PBS buffer were used as the positive and negative control. The change of fluorescence was monitored using a fluorescent microplate reader (excitation 622 nm, emission 670 nm).

### **9. Zeta potential measurements**

Bacterial solutions of *E. coli* or *S. aureus* was added into a 96-well plate and mixed with **H**, **G** and **HG**, respectively, and incubated for 3 h. The bacterial suspensions were further centrifuged for 5 min (8000 rpm) to remove the supernatant. Then, the precipitate was added with deionized water for the zeta potential measurements. *E. coli* or *S. aureus* with 1% TX-100 and PBS buffer were used as the positive and negative controls.

### **10. N-phenyl-naphthylamine (NPN) uptake assay**

Bacteria suspension of *E. coli* (OD<sub>600</sub> = 0.34) was prepared to carry out the NPN assay. 160  $\mu$ L of the bacterial suspension was transferred into the wells of a 96-well plate. Then, PBS (18  $\mu$ L) and NPN dye (40 mM, 2  $\mu$ L) were added to the wells containing *E. coli* bacterial suspension and pre-incubated for about 5 min. After the incubation, fluorescence was monitored using a fluorescent microplate reader (excitation 350 nm, emission 420 nm). Then, 20  $\mu$ L of **HG** was added and incubated for 180 min. The change in fluorescence was monitored by a microplate reader. Triton X-100 (1%) in PBS was used as the positive control and pure PBS was used as the negative control, respectively.

### 11. Propidium iodide (PI) uptake assay

Inner membrane permeability assays with the propidium iodide (PI) probe were performed. 80  $\mu\text{L}$  of the bacterial suspension of *E. coli* or *S. aureus* ( $\text{OD}_{600} = 0.34$ ) was transferred into the wells of a 96-well plate. Then, PI dye (400  $\mu\text{M}$ , 40  $\mu\text{L}$ ) was added to the wells containing *E. coli* or *S. aureus* bacterial suspension and pre-incubated for about 5 min. After the incubation, fluorescence was monitored using a fluorescent microplate reader (excitation 535 nm, emission 617 nm). Then, 80  $\mu\text{L}$  of **H**, **G** and **HG**, respectively, were added, and changes in fluorescence were monitored by a microplate reader. Triton X-100 (1%) in PBS was used as the positive control and pure PBS was used as the negative control, respectively.

### 12. Protein and DNA leakage assays

*E. coli* and *S. aureus* bacterial suspension were treated with **H**, **G** and **HG** for 3 h, respectively. These aqueous suspensions of bacterial cells were centrifuged, filtered with a membrane (0.22  $\mu\text{m}$ ), and the supernatants were collected. *E. coli* and *S. aureus* cells with 1% TritonX-100 and PBS buffer were used as the positive and negative control, respectively. The protein contents in the supernatants were measured using an enhanced BCA protein assay kit. The absorbance intensity at 562 nm was recorded by a microplate reader and the protein concentrations were calculated against a standard calibration curve using bovine serum albumin (BSA) as a model protein. DNA concentrations were quantified by measuring the optical values of the collected supernatants at the wavelength of 260 nm ( $\text{OD}_{260}$ ).

### 13. Hemolysis assay

The hemolytic activities of **H**, **G** and **HG** were tested using Rat red blood cells (2%). **H**, **G** and **HG** were serially diluted to different concentrations. Triton X-100 (1%) in PBS was used as the positive control and pure PBS was used as the negative control, respectively. After mixing an equal volume of erythrocyte suspension and tested compounds, the cells were incubated at 37  $^{\circ}\text{C}$  for 3 h. After centrifugation at 2000 rpm for 10 min, the supernatant (100  $\mu\text{L}$ ) was transferred to a 96-well plate, and the

absorbance at 576 nm was collected by a microplate reader to calculate the percentage of hemolysis using the following equation:

$$\text{Hemolysis\%} = (A_{\text{sample}} - A_{\text{negative control}}) / (A_{\text{positive control}} - A_{\text{negative control}}) \times 100\%$$

Where  $A_{\text{sample}}$  is the absorbance of the compound to be measured,  $A_{\text{positive control}}$  is the absorbance in the presence of Triton X-100, and  $A_{\text{negative control}}$  is the absorbance in the presence of PBS.

#### 14. Cell viability assay

The cytotoxicities of **H**, **G** and **HG** were evaluated by Cell Counting Kit-8 (CCK8, APEX-BIO) assay. HaCat cells (HTX2089, Otwo Biotech) were seeded into 96-well plates at a concentration of  $10^4$  cells per well. After 24 h incubation, the culture medium was removed and replaced with 100  $\mu\text{L}$  of fresh medium containing PBS, **H**, **G** and **HG**, respectively. The cells were incubated for 24 h. Then, each well was replaced by 100  $\mu\text{L}$  of fresh medium added with 10  $\mu\text{L}$  of CCK-8 reagent. After 2 h of incubation, the optical density was measured at 450 nm by a spectrophotometer. The percentage of cell viability was calculated using the following equation:

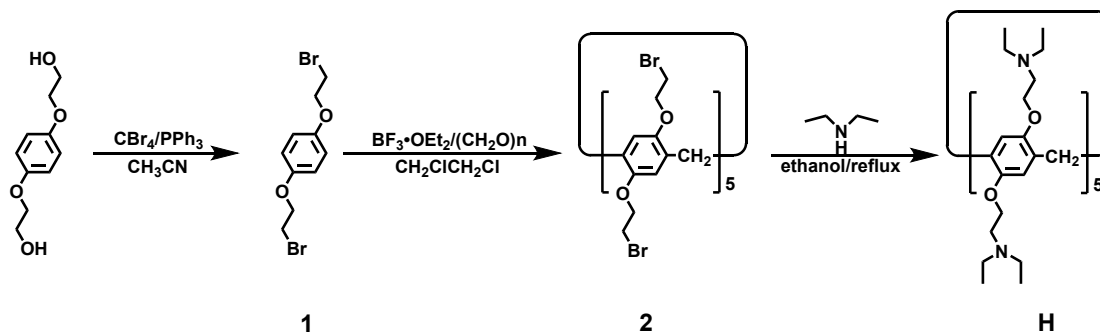
$$\text{Cell viability\%} = (A_{\text{sample}} - A_{\text{blank}}) / (A_{\text{control}} - A_{\text{blank}}) \times 100\%$$

Where  $A_{\text{sample}}$  is the absorbance in the presence of tested compounds after 24 h incubation;  $A_{\text{control}}$  is the absorbance in the presence of tested compounds at 0 h;  $A_{\text{blank}}$  is the absorbance in the presence of PBS.

#### 15. Statistical analysis

Data are represented as mean  $\pm$  standard deviation (S.D). Group differences were conducted by one-way ANOVA with Tukey's post-hoc test.  $P$ -values  $< 0.05$  were considered as statistically significant ( $*p < 0.05$ ,  $**p < 0.01$ ,  $***p < 0.001$ ,  $****p < 0.0001$ ). All statistical analyses were performed with GraphPad Prism 8.





**Scheme S1.** Synthesis of diethylamine pillar[5]arene **H**.

Tetrabromomethane (29.85 g, 90.00 mmol) was gradually added to a mixture of 1,4-bis(2-hydroxyethoxy)benzene (7.93 g, 40.00 mmol) and triphenylphosphine (23.61g, 90.00 mmol) in acetonitrile (250 mL) at 0 °C. After the solid was dissolved completely, the mixture solution was further stirred for 5 h at room temperature. The reaction solution was poured into cold water (500 mL) to generate white precipitate. The precipitate was collected by filtration and washed several times with methanol/water (v/v, 3/1) to afford compound **1** as white solid (8.76 g, yield: 67.6 %). The  $^1\text{H}$  NMR spectrum of **1** is shown in Fig. S1.  $^1\text{H}$  NMR (400 MHz,  $\text{CDCl}_3$ , 298K)  $\delta$  (ppm): 6.86 (s, 4H), 4.24 (t,  $J = 6.3$  Hz, 4H), 3.62 (t,  $J = 6.3$  Hz, 4H).

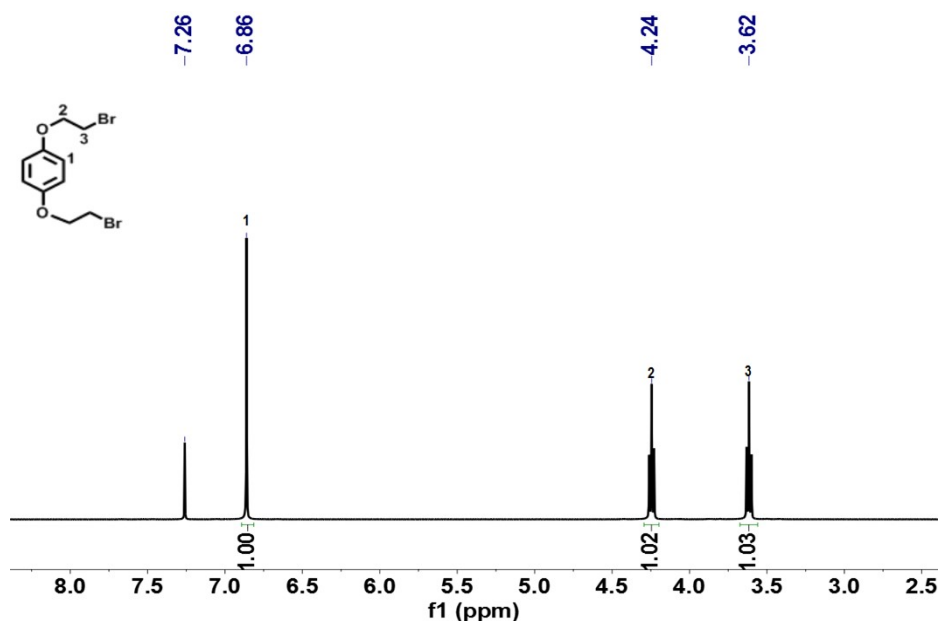


**Fig. S1**  $^1\text{H}$  NMR spectrum of compound **1** (400 MHz,  $\text{CDCl}_3$ , 298K).

A mixture of 1,4-bis(2-bromoethoxy)benzene (10.37 g, 32.00 mmol), potassium carbonate (2.89 g, 96.00 mmol) and 1,2-dichloroethane (300 mL) was added to a 500 mL round bottom flask. Then, boron trifluoride diethyl etherate complex (9.37 mL, 74.00 mmol) was injected into the solution. After stirred at room temperature for 3-5 h, it was quenched by water. The organic layer was extracted to afford a crude product, which was further purified by column chromatography with petroleum ether/dichloromethane (v/v, 1/4) to obtain compound 2 as a white solid (1.04 g, yield: 30.4%). The  $^1\text{H}$  NMR spectrum of 2 is shown in Fig. S2.  $^1\text{H}$  NMR (400 MHz,  $\text{CDCl}_3$ , 298 K)  $\delta$  (ppm): 6.91 (s, 10H), 4.23 (t,  $J = 5.6$  Hz, 20H), 3.84 (s, 10H), 3.63 (t,  $J = 5.6$  Hz, 20H).

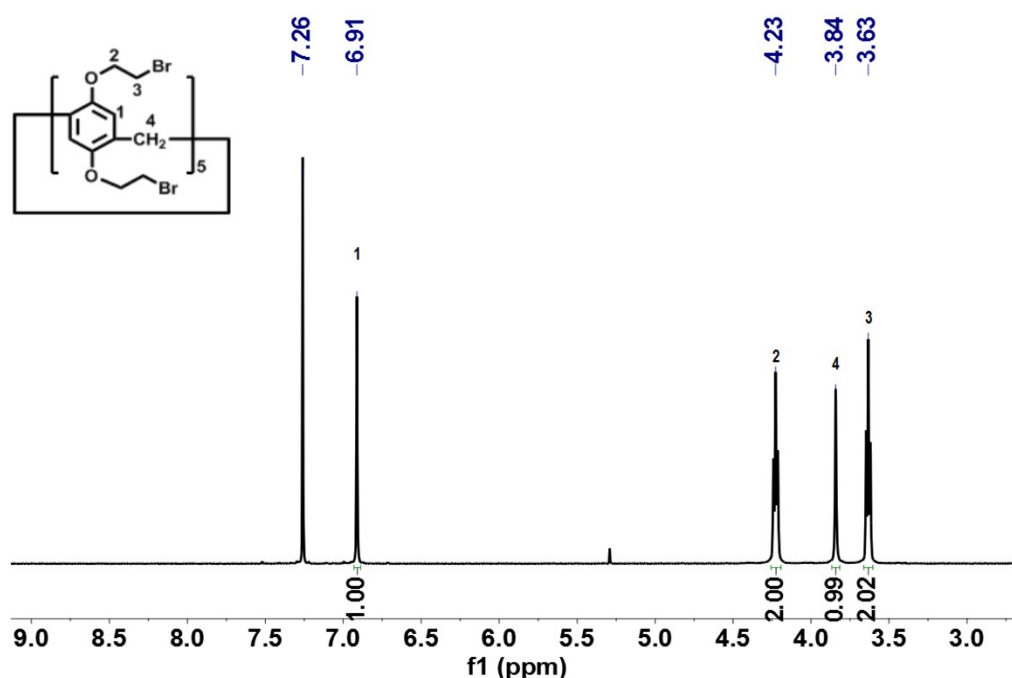


**Fig. S2**  $^1\text{H}$  NMR spectrum of compound 2 (400 MHz,  $\text{CDCl}_3$ , 298K).

Compound 2 (1.00 g, 0.57 mmol) and diethylamine (4.00 mL, 85.21 mmol) were dissolved in ethanol (100 mL) and refluxed at 90 °C for 3 d. The solution was dried under vacuum to afford a crude product. Then, it was dissolved in dichloromethane and washed with saturated potassium carbonate solution. The organic phase is extracted to obtain compound **H** as a dark brown oily solid (0.71 g, yield: 77.2%). The  $^1\text{H}$  NMR spectrum of **H** is shown in Fig. S3.  $^1\text{H}$  NMR (400 MHz,  $\text{CDCl}_3$ , 298 K)  $\delta$ (ppm): 6.85

(s, 10H), 4.14–3.84 (m, 20H), 3.74 (s, 10H), 3.03–2.83 (m, 20H), 2.65 (q,  $J = 7.1$  Hz, 40H), 1.05 (t,  $J = 7.1$  Hz, 60H).

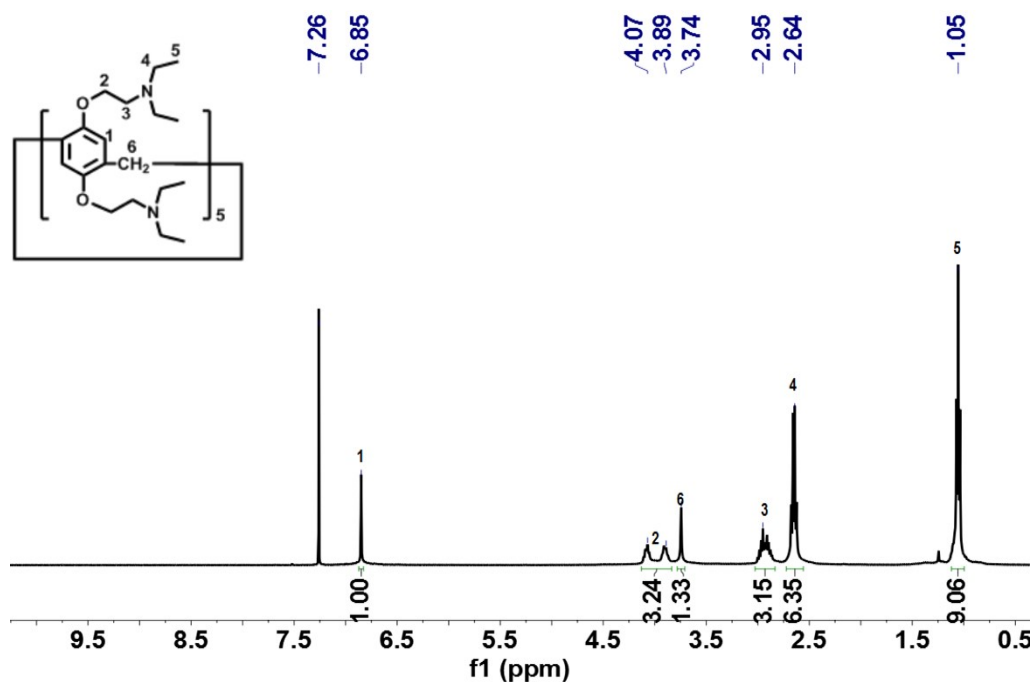
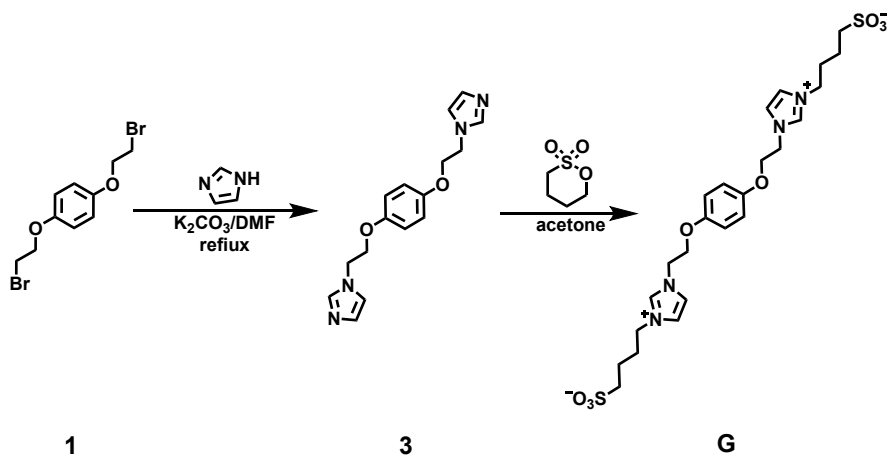


**Fig. S3**  $^1\text{H}$  NMR spectrum of compound **H** (400 MHz,  $\text{CDCl}_3$ , 298K).



**Scheme S2.** Synthesis of zwitterionic guest molecule **G**.

A mixture of compound **1** (4.02 g, 12.41 mmol), imidazole (5.07 g, 74.44 mmol) and potassium carbonate (10.29 g, 74.44 mmol) was refluxed in  $\text{N,N}$ -dimethylformamide (100 mL) at  $80^\circ\text{C}$  for 3 d. After remove the solvent, the crude product was washed with water for 3 times to obtain compound **3** as a white solid (2.98 g, yield: 80.5%). The  $^1\text{H}$

NMR spectrum of **3** is shown in Fig. S4.  $^1\text{H}$  NMR (400 MHz,  $\text{CDCl}_3$ , 298 K)  $\delta$  (ppm): 7.57 (s, 2H), 7.05 (s, 2H), 7.01 (s, 2H), 6.76 (s, 4H), 4.28 (t,  $J = 5.1$  Hz, 4H), 4.14 (t,  $J = 5.1$  Hz, 4H).

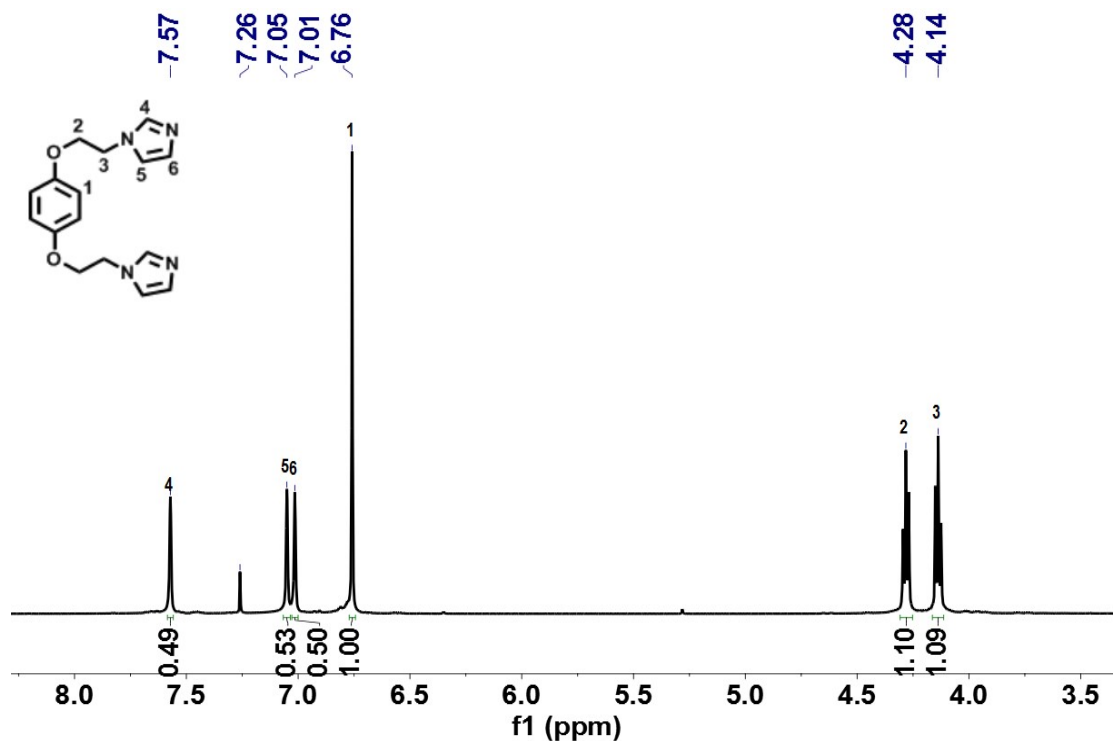


Fig. S4  $^1\text{H}$  NMR spectrum of compound **3** (400 MHz,  $\text{CDCl}_3$ , 298K).

A mixture of compound **3** (1.00 g, 3.35 mM) and 1,4-butane sultone (0.73 mL, 7.37 mM) was dissolved in acetone (50 mL) and stirred at room temperature for 5 d under  $\text{N}_2$  atmosphere. The precipitate was collected by filtration and washed several times with dichloromethane and ethyl acetate to obtain compound **G** as a white solid (1.34 g, yield: 70.1%). The  $^1\text{H}$  NMR spectrum of **G** is shown in Fig. S5.  $^1\text{H}$  NMR (400 MHz,  $\text{D}_2\text{O}$ , 298K)  $\delta$  (ppm): 8.87 (s, 2H), 7.56 (s, 2H), 7.48 (s, 2H), 6.87 (s, 2H), 4.59–4.52 (m, 4H), 4.40–4.33 (m, 4H), 4.20 (t,  $J = 7.0$  Hz, 4H), 2.91–2.82 (m, 4H), 1.93 (dt,  $J = 15.3, 7.3$  Hz, 4H), 1.65 (dt,  $J = 15.2, 7.4$  Hz, 4H). The  $^{13}\text{C}$  NMR spectrum of **G** is shown in Fig. S6.  $^{13}\text{C}$  NMR (100 MHz,  $\text{D}_2\text{O}$ , 298 K)  $\delta$  (ppm): 152.73, 123.60, 122.17, 68.93, 49.51, 35.77, 29.38, 28.33, 25.52. HRESIMS:  $m/z$  calcd for  $[\text{M} + \text{Na}]^+$   $\text{C}_{24}\text{H}_{34}\text{N}_4\text{O}_8\text{S}_2\text{Na}$  593.17; found 593.1012, error  $-0.1$  ppm.

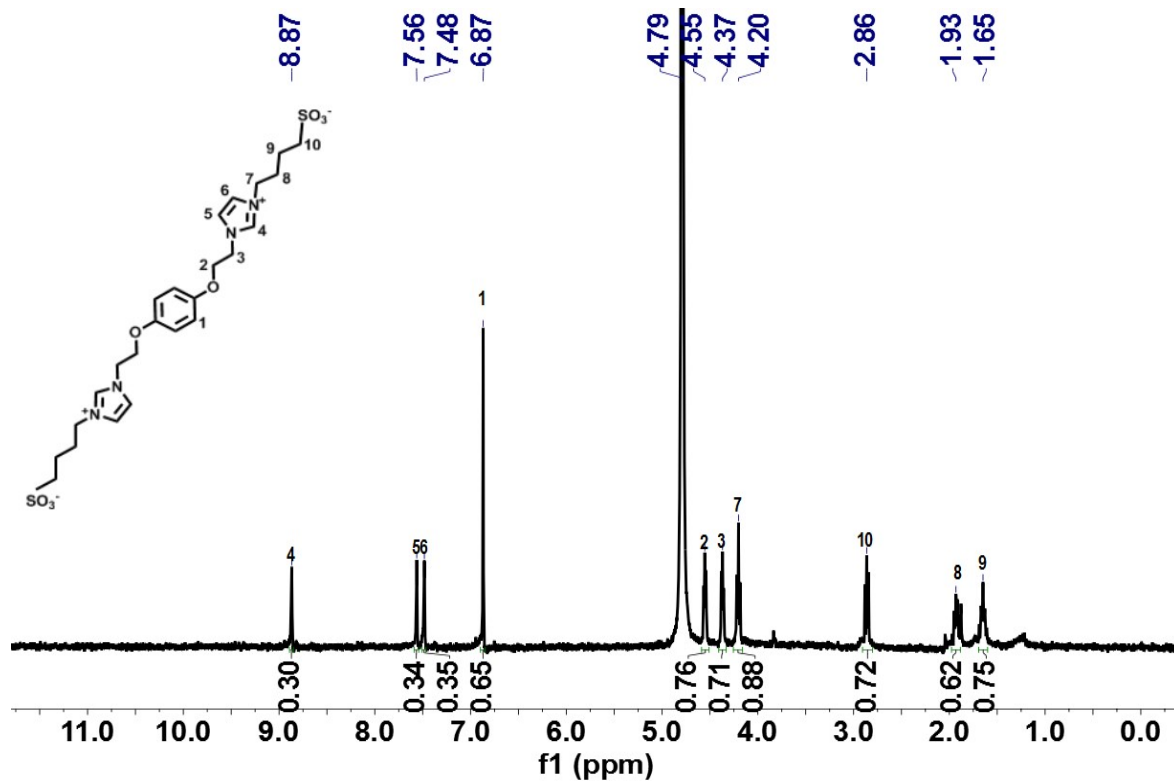


Fig. S5  $^1\text{H}$  NMR spectrum of compound G (400 MHz,  $\text{D}_2\text{O}$ , 298K).

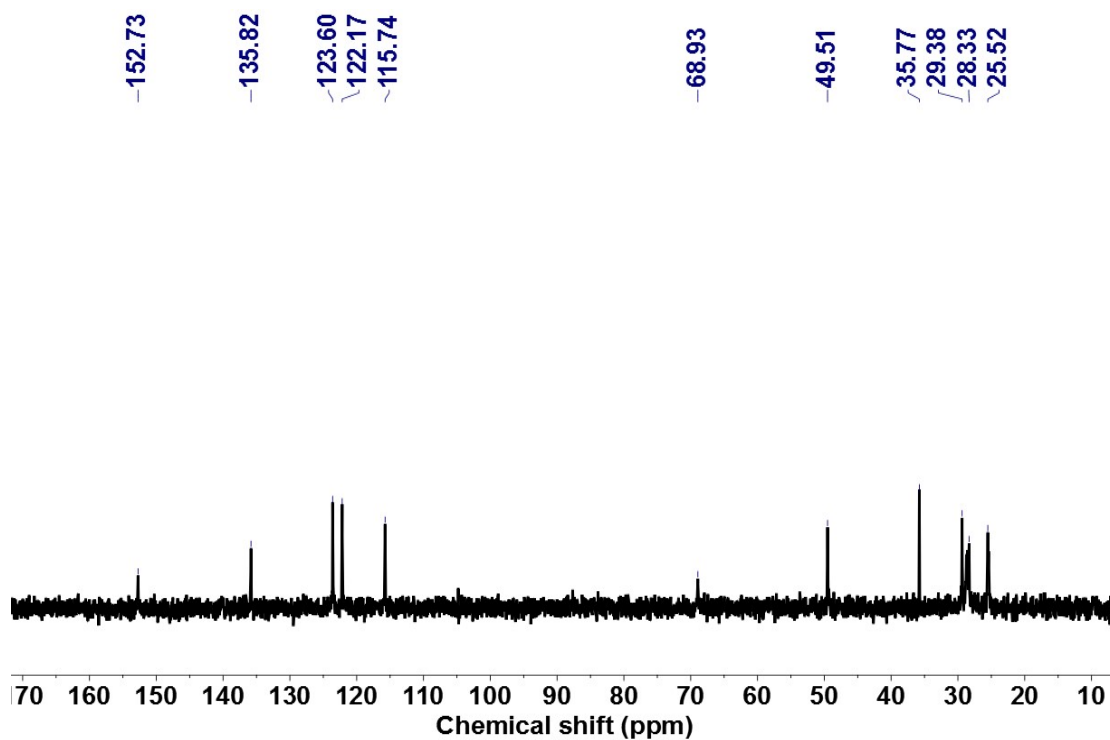
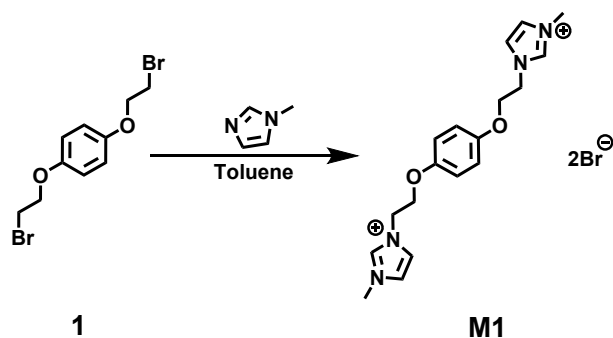
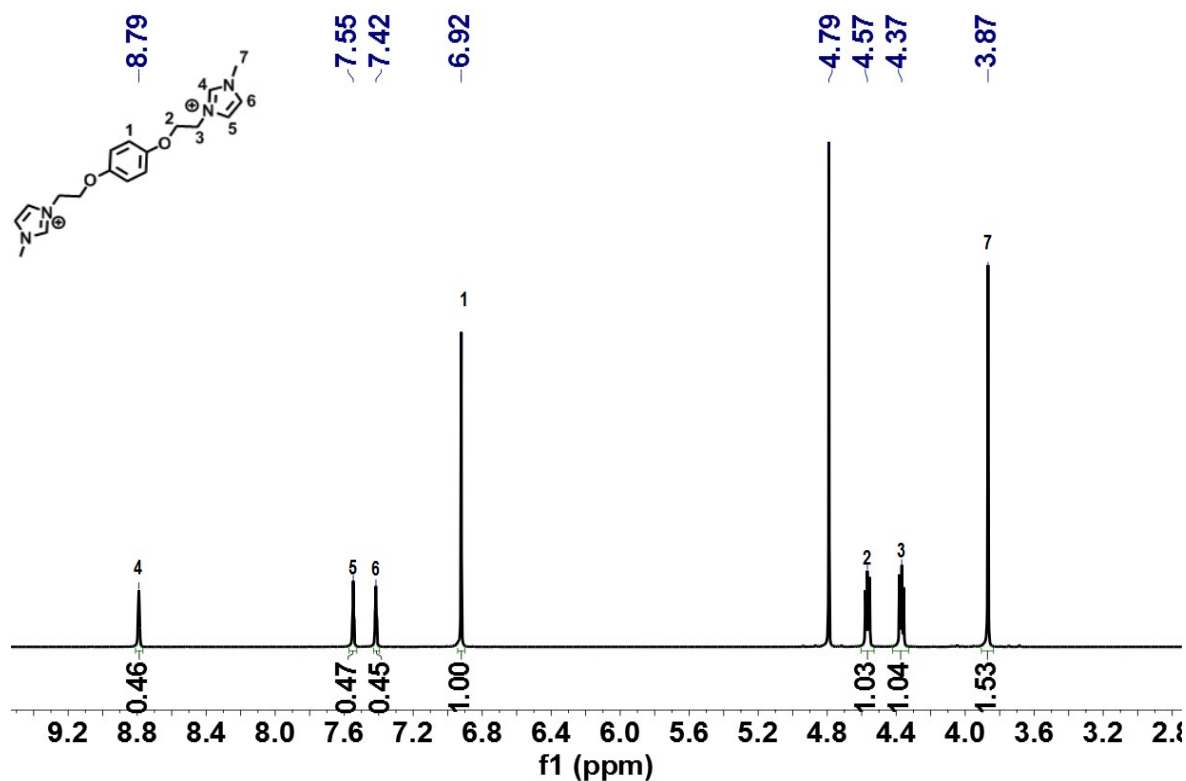


Fig. S6  $^{13}\text{C}$  NMR spectrum of compound G (100 MHz,  $\text{D}_2\text{O}$ , 298K).

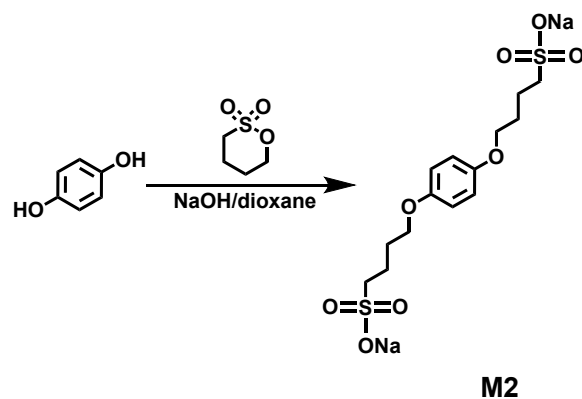


**Scheme S3.** Synthesis of model molecule **M1**.

A mixture of **1** (1.68 g, 5.00 mmol) and N-methylimidazole (1.64 g, 20.0 mmol) were dissolved in toluene (25 mL) and stirred at 120 °C for 24 h. After cooling, the solvent was removed and the residue was recrystallized from ethanol/diethyl ether (v:v, 1:2) to give a white solid (1.48 g, yield: 90%). The <sup>1</sup>H NMR spectrum of **M1** is shown in Fig. S7. <sup>1</sup>H NMR (400 MHz, D<sub>2</sub>O, 298K) δ (ppm): 8.79 (s, 2H), 7.55 (t, *J* = 1.7 Hz, 2H), 7.42 (t, *J* = 1.4 Hz, 2H), 6.92 (s, 4H), 4.60-4.53 (m, 4H), 4.42-4.33 (m, 4H), 3.87 (s, 6H).



**Fig. S7** <sup>1</sup>H NMR spectrum of compound **M1** (400 MHz, D<sub>2</sub>O, 298K).



**Scheme S4.** Synthesis of model molecule **M2**.

A solution of butanesultone (2.45 g, 20.00 mmol) in 1,4-dioxane (20 mL) was added into a solution of hydroquinone (0.88 g, 8.00 mmol) in aqueous NaOH solution (10 wt%, 20 mL). The mixture was stirred at RT. for 12 h then filtered to collect the crude solid. The solid was stirred with acetone (200 mL) then dried under high vacuum to yield **M2** as a white solid (2.49 g, yield: 80%). The  $^1\text{H}$  NMR spectrum of **M2** is shown in Fig. S8.  $^1\text{H}$  NMR (400 MHz,  $\text{D}_2\text{O}$ , 298K)  $\delta$  (ppm): 6.98 (s, 4H), 4.06 (t,  $J = 5.9$  Hz, 4H), 2.96 (t,  $J = 7.5$  Hz, 4H), 1.87 (dt,  $J = 6.7, 3.2$  Hz, 8H).

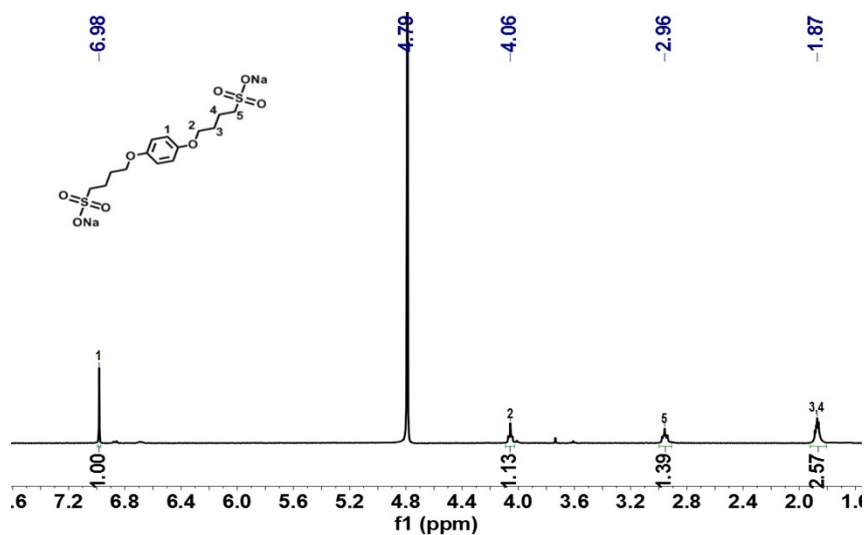


**Fig. S8**  $^1\text{H}$  NMR spectrum of compound **M2** (400 MHz,  $\text{D}_2\text{O}$ , 298K).

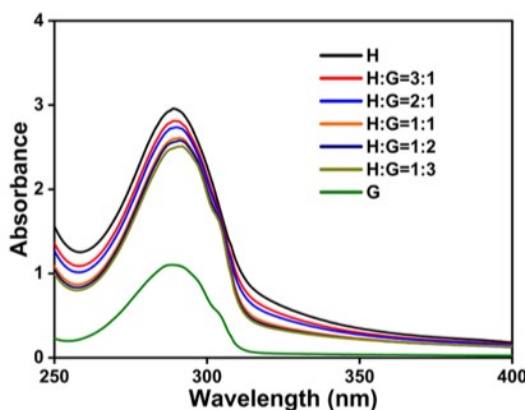


Fig. S9 a) UV-vis spectra of **H** and **G** in water with different proportions.

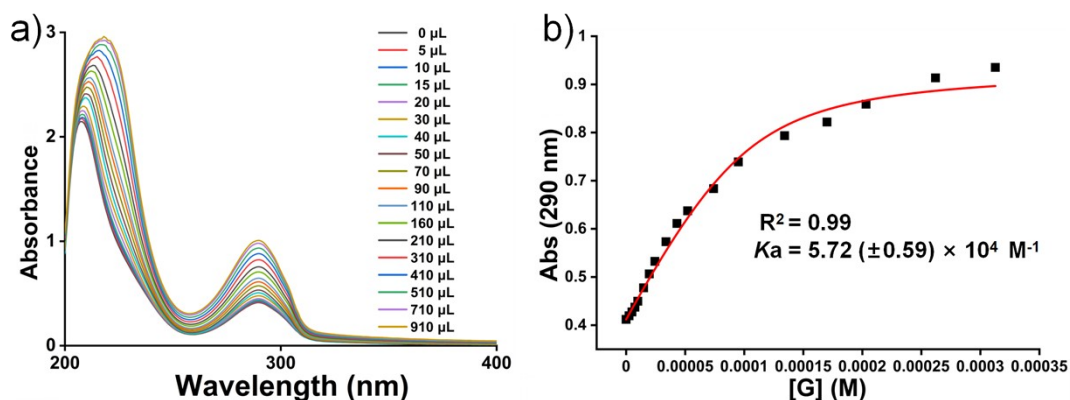
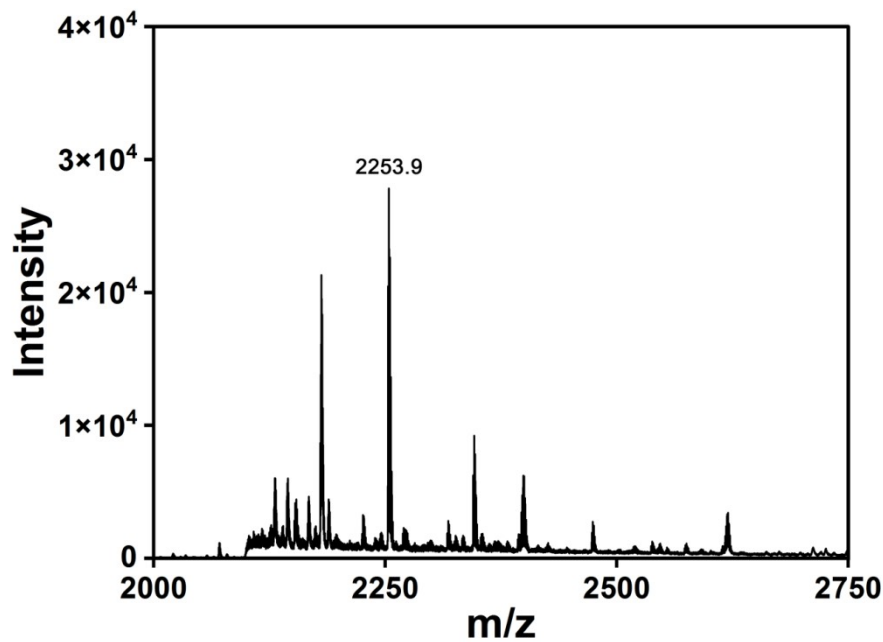


Fig. S10 a) The UV-vis absorption spectra of **H** ( $\text{H}_2\text{O}$ , 298 K,  $5 \times 10^{-5}$  M) upon addition of **G** ( $\text{H}_2\text{O}$ , 298 K,  $5 \times 10^{-3}$  M). b) The red solid line was obtained from the non-linear curve-fitting.

UV-vis titration was done with solution which had a constant concentration of **H** (0.00005 mM) and varying concentrations of **G**. The UV-vis absorption spectra of **H** upon addition of **G** was shown in Fig. S10a. From the titration result, the association constant ( $K_a$ ) of **H** + **G** was estimated to be about  $5.72 (\pm 0.59) \times 10^4 \text{ M}^{-1}$  by a non-linear curve-fitting method.<sup>S3</sup>





**Fig. S11** Electrospray ionization mass spectrum of **HG**. Main peak:  $m/z$  2253.9 [ $M + \text{CH}_3\text{OH} + \text{K}]^+$  (100%).

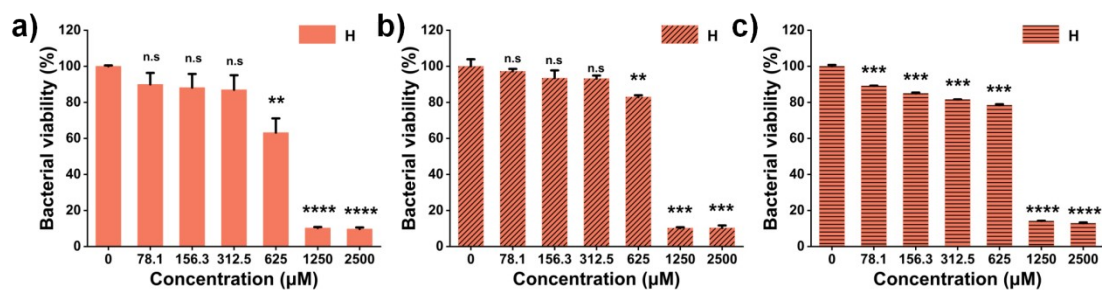


**Fig. S12** Antibacterial activity of **H** against a) *E. coli*, b) *S. aureus* and c) MRSA (n.s. indicates not significant;  $P$ -values  $< 0.05$  were considered statistically significant, \*\* $p < 0.01$ , \*\*\* $p < 0.001$ , \*\*\*\* $p < 0.001$ ).

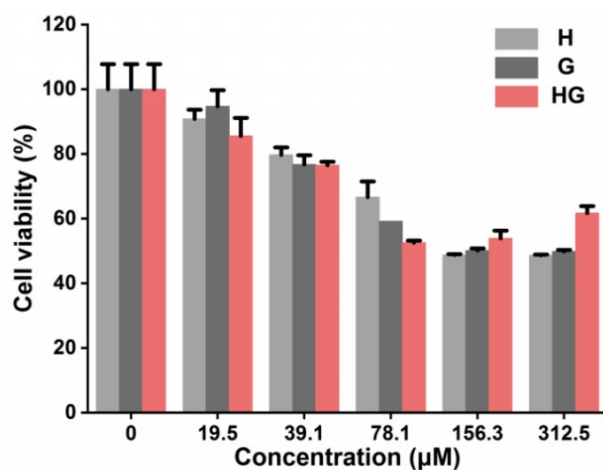


**Fig. S13** Cell viability of HaCat cells incubated with different concentrations of **H**, **G** and **HG**.

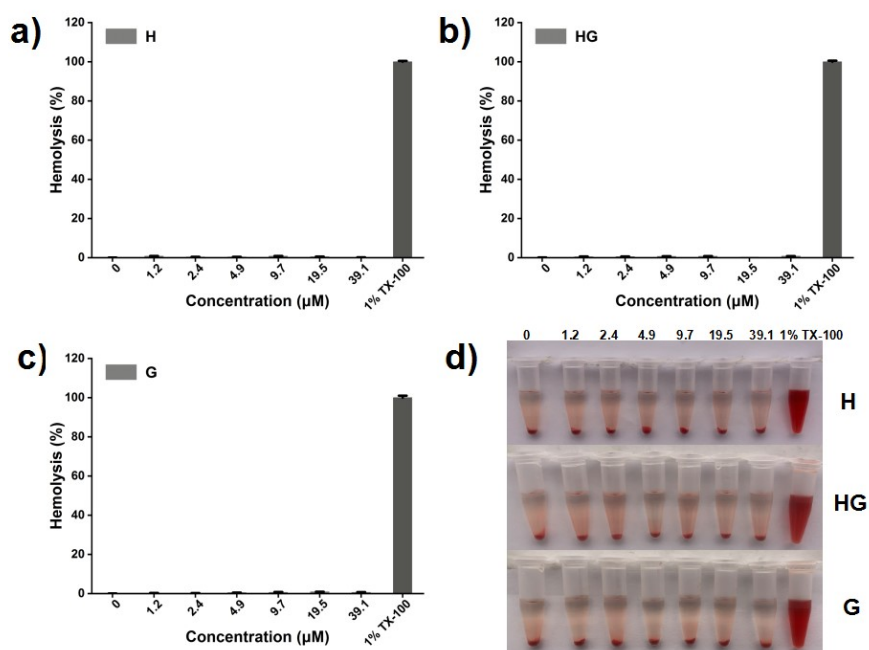


**Fig. S14** Hemolytic assay of rat red blood cells in the presence of a) **H**, b) **HG**, c) **G** and d) corresponding photos.

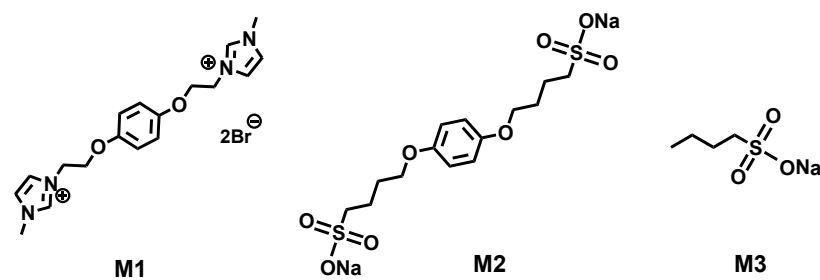


**Fig. S15** Chemical structures of truncated guest molecules **M1**, **M2** and **M3**.

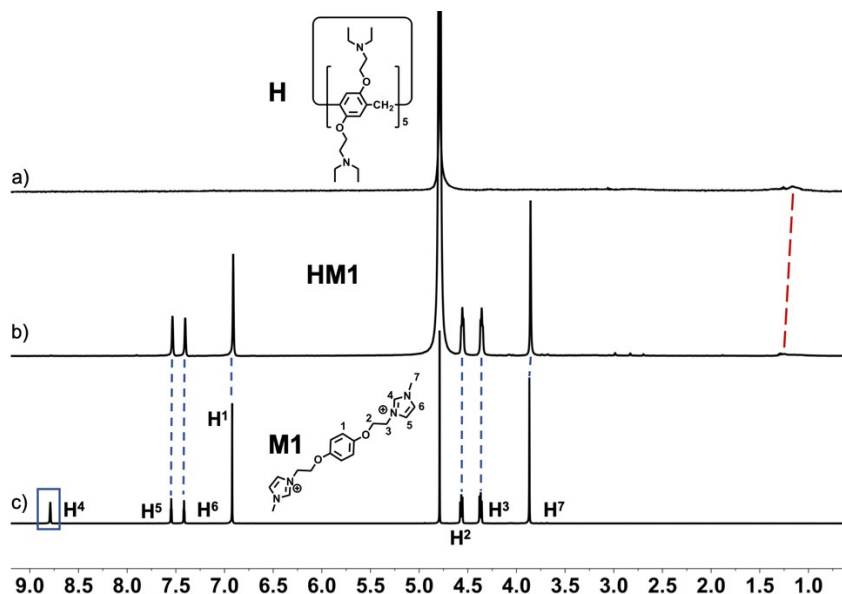


**Fig. S16**  $^1\text{H}$  NMR spectra of (a) **H**, (b) **HM1** complex and (c) **M1** (400 MHz,  $\text{D}_2\text{O}$ , 298K).

From the  $^1\text{H}$  NMR spectra, the signal of  $\text{H}_4$  on the imidazole ring disappears due to the complexation-induced broadening effects, the peaks of protons  $\text{H}_2$ ,  $\text{H}_3$ ,  $\text{H}_5$ ,  $\text{H}_6$  and  $\text{H}_7$  on **M1** exhibit slight upfield shifts, indicating the formation of host–guest complex in solution.

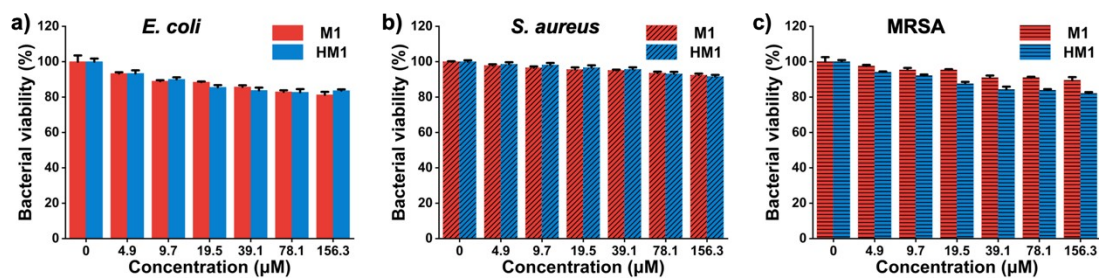


**Fig. S17** Antibacterial activity of **M1** and **HM1** against a) *E. coli*, b) *S. aureus* and c) MRSA.

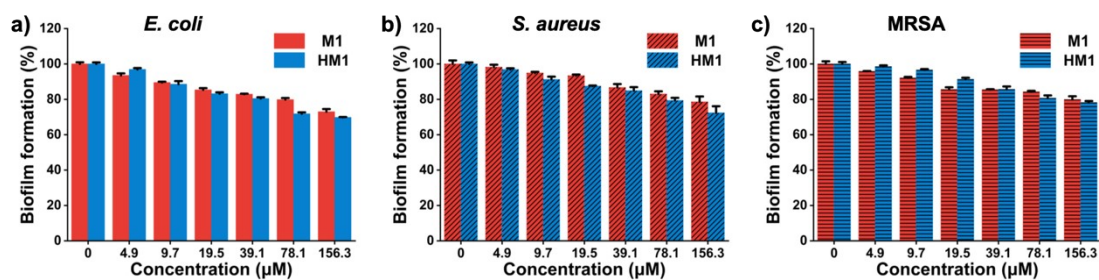


**Fig. S18** Biofilm inhibitory effects of **M1** and **HM1** complex against a) *E. coli*, b) *S. aureus* and c) MRSA.

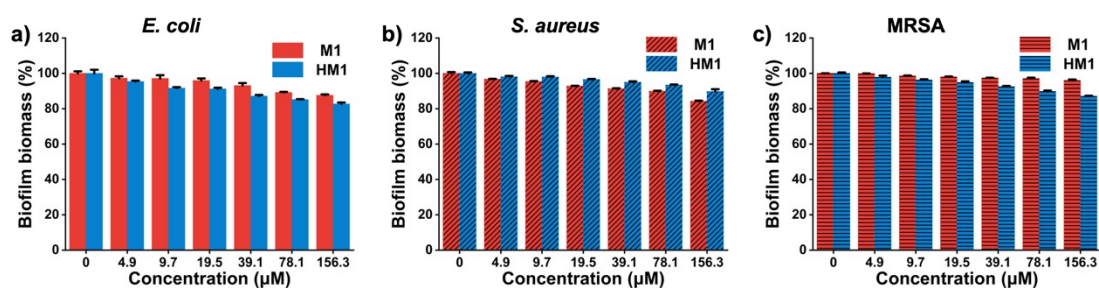


**Fig. S19** Quantification of the biofilm biomass of **M1** and **HM1** complex against a) *E. coli*, b) *S. aureus* and c) MRSA.

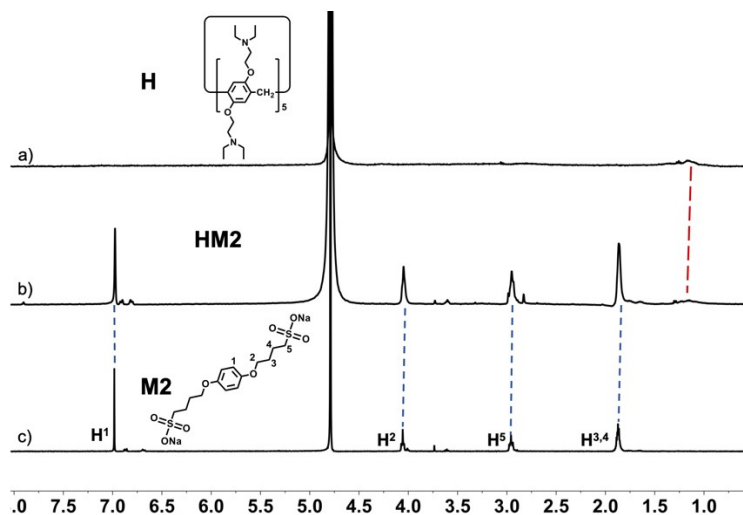


**Fig. S20** <sup>1</sup>H NMR spectra of (a) **H**, (b) **HM2** complex and (c) **M2** (400 MHz, D<sub>2</sub>O, 298K).

From the <sup>1</sup>H NMR spectra, the peaks of protons H<sub>1</sub>, H<sub>2</sub>, H<sub>3</sub>, H<sub>4</sub> and H<sub>5</sub> on **M2** exhibit slight upfield shifts, indicating the formation of host-guest complex in solution.

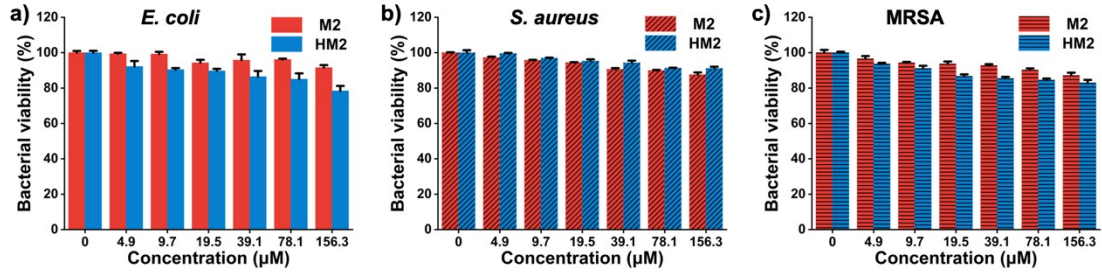


**Fig. S21** Antibacterial activity of M2 and HM2 against a) *E. coli*, b) *S. aureus* and c) MRSA.

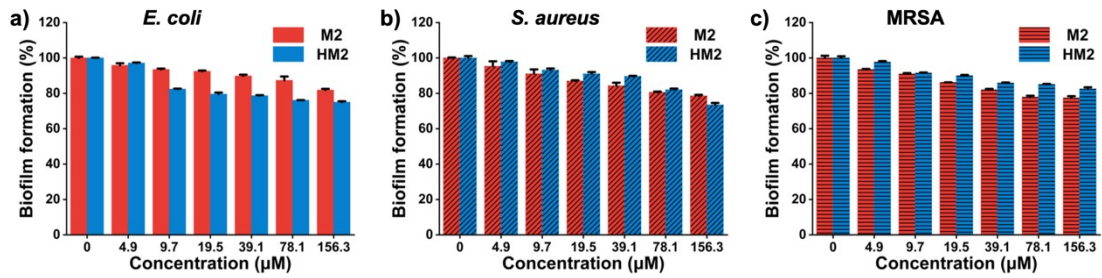


**Fig. S22** Biofilm inhibitory effects of M2 and HM2 complex against a) *E. coli*, b) *S. aureus* and c) MRSA.

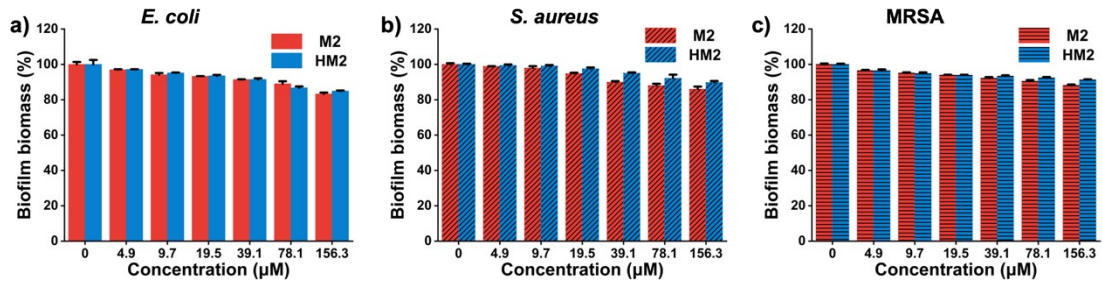


**Fig. S23** Quantification of the biofilm biomass of M2 and HM2 complex against a) *E. coli*, b) *S. aureus* and c) MRSA.

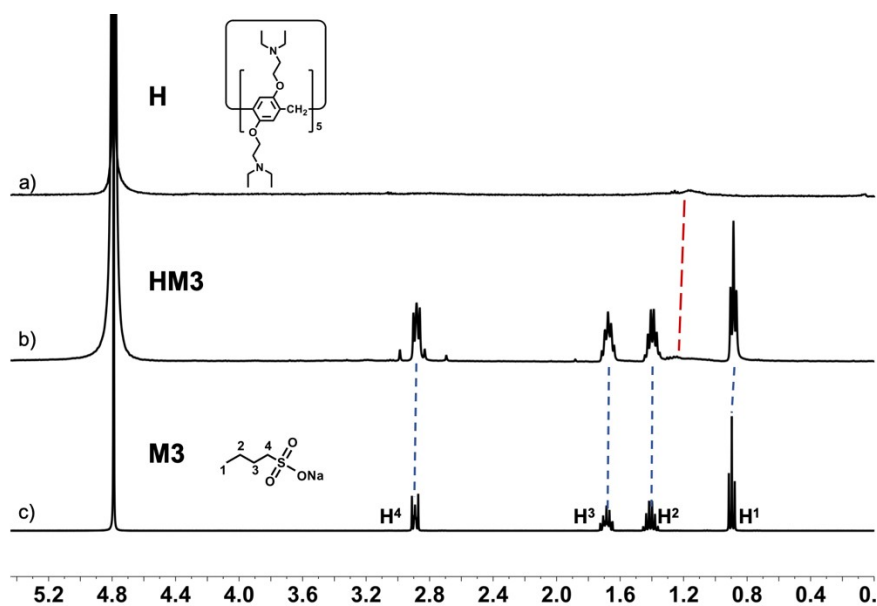


**Fig. S24**  $^1\text{H}$  NMR spectra of (a) **H**, (b) **HM3** complex and (c) **M3** (400 MHz,  $\text{D}_2\text{O}$ , 298K).

From the  $^1\text{H}$  NMR spectra, the peaks of protons  $\text{H}_1$ ,  $\text{H}_2$ ,  $\text{H}_3$  and  $\text{H}_4$  on **M3** exhibit slight upfield shifts, indicating the formation of host-guest complex in solution.

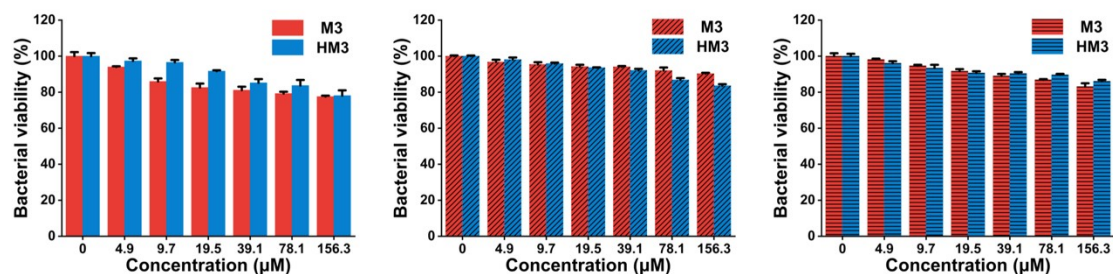


**Fig. S25** Antibacterial activity of **M3** and **HM3** against a) *E. coli*, b) *S. aureus* and c) MRSA.

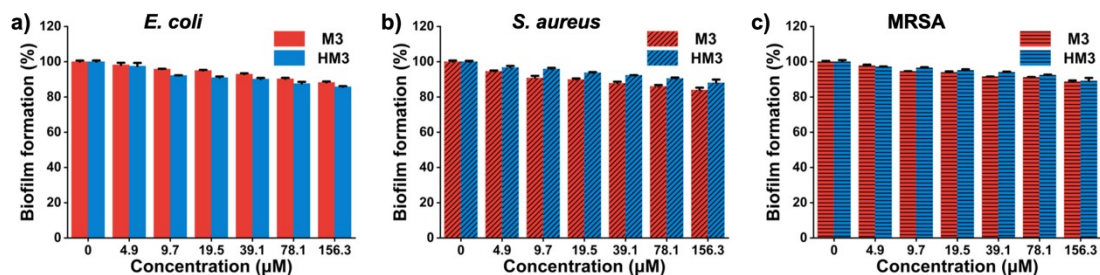


**Fig. S26** Biofilm inhibitory effects of **M3** and **HM3** complex against a) *E. coli*, b) *S. aureus* and c) MRSA.

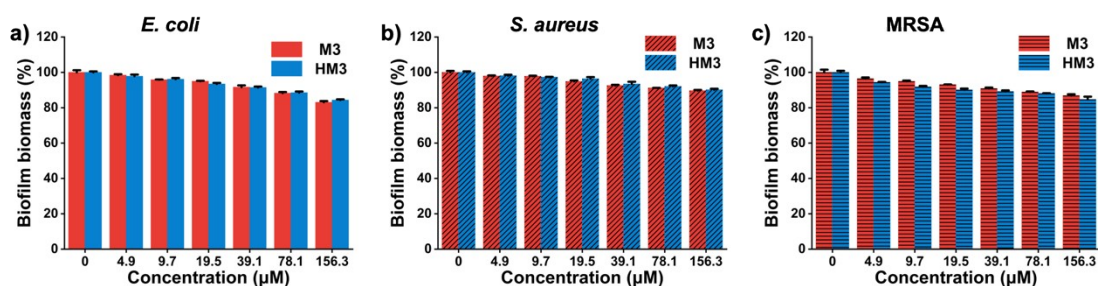


**Fig. S27** Quantification of the biofilm biomass of **M3** and **HM3** complex against a) *E. coli*, b) *S. aureus* and c) MRSA.

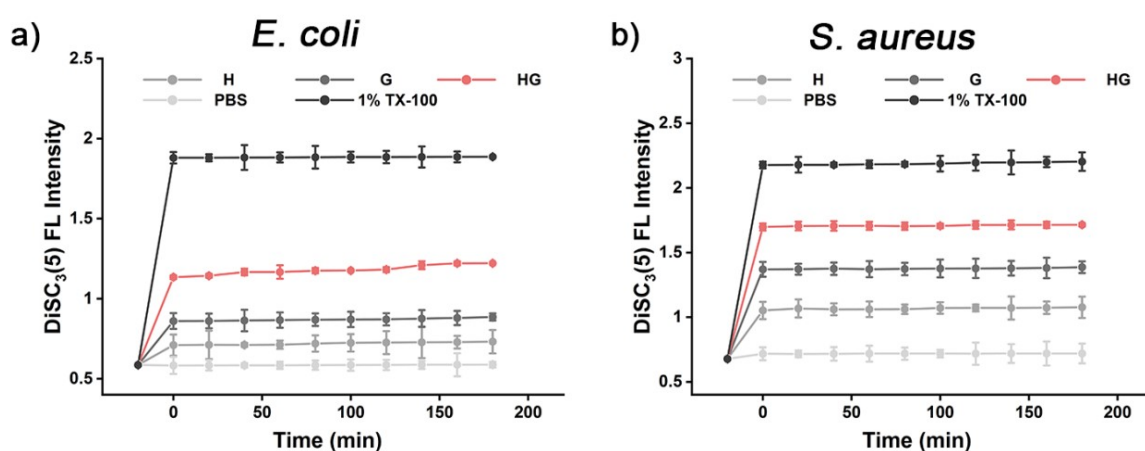


**Fig. S28** Cytoplasmic membrane potential assay of a) *E. coli* and b) *S. aureus* incubated with H, G and HG, respectively ( $[\text{H}] = [\text{G}] = [\text{HG}] = 39.1 \mu\text{M}$ ). 1% TX-100 and PBS buffer were used as the positive and negative control.

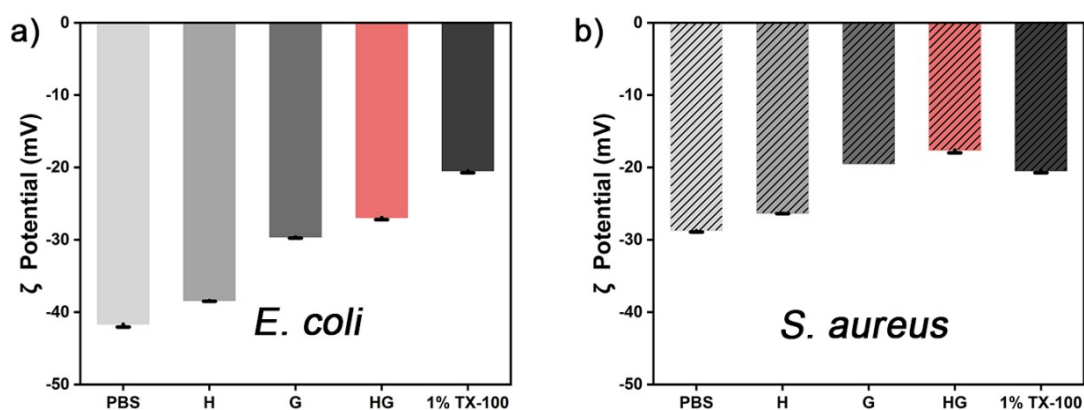


**Fig. S29**  $\zeta$ -potentials of a) *E. coli* and b) *S. aureus* incubated with H, G and HG, respectively ( $[\text{H}] = [\text{G}] = [\text{HG}] = 39.1 \mu\text{M}$ ).

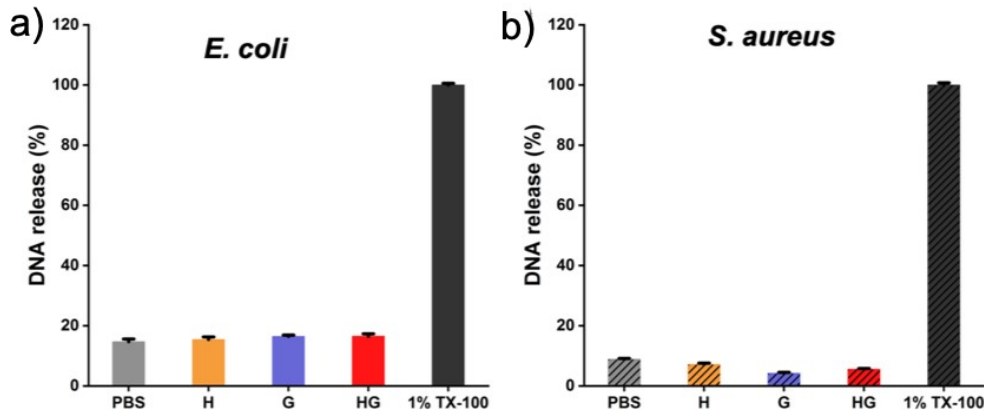


**Fig. S30** DNA release assays of *E. coli* and *S. aureus* incubated with **H**, **G** and **HG**, respectively ( $[H] = [G] = [HG] = 39.1 \mu\text{M}$ ).

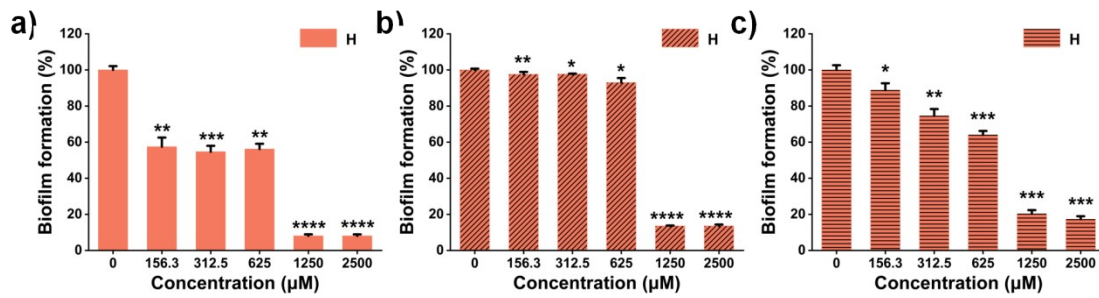


**Fig. S31** Biofilm inhibitory effect of **H** against a) *E. coli*, b) *S. aureus* and c) MRSA. ( $P$ -values  $< 0.05$  were considered as statistically significant,  $*p < 0.05$ ,  $**p < 0.01$ ,  $***p < 0.001$ ,  $****p < 0.0001$ .)

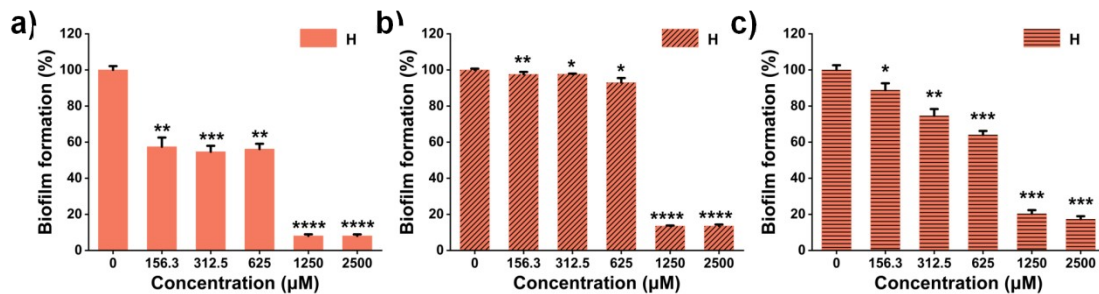


**Fig. S32** Quantification of the biofilm biomass of **H** against a) *E. coli*, b) *S. aureus* and c) MRSA. (n.s. indicates not significant,  $P$ -values  $< 0.05$  were considered as statistically significant,  $*p < 0.05$ ,  $**p < 0.01$ ,  $***p < 0.001$ ).



## Reference

- S1. H. Yang, L. Jin, D. Zhao, Z. Lian, M. Appu, J. Huang and Z. Zhang, *J. Agric. Food Chem.*, 2021, **69**, 4276–4283.
- S2. M. Yoshizawa, M. Hirao, K. Ito-Akita and H. Ohno, *J. Mater. Chem.*, 2001, **11**, 1057–1062.
- S3. M. Liu, X. Yan, M. Hu, X. Chen, M. Zhang, B. Zheng, X. Hu, S. Shao and F. Huang, *Org. Lett.*, 2010, **12**, 2558-2561.